

# Experimental Evaluation of TiN Coating on Fouling Resistance of PWR Fuel Cladding

Junhyuk Ham <sup>a</sup>, Yunju Lee <sup>a</sup>, Seung Chang Yoo <sup>a</sup>, and Ji Hyun Kim <sup>a\*</sup>

<sup>a</sup>Department of Nuclear Engineering, School of Mechanical, Aerospace, and Nuclear Engineering, Ulsan National Institute of Science and Technology, 50 UNIST-gil, Ulsan, 44919, Republic of Korea

\*Corresponding author: kimjh@unist.ac.kr

## 1. Introduction

As the fuel cycle in commercial nuclear power plants has been extended, some undesirable deposits have occurred on the upper side of fuel cladding surfaces, as observed in the Callaway pressurized water reactor (PWR) in the United States during its 9<sup>th</sup> cycle [1]. This problem is caused by a combination of heat transfer and corrosion phenomena. According to the direction of coolant flow through the fuel assembly, the surface temperature on the upper side of the cladding is higher than on the lower side. When the surface temperature increases above the coolant saturation temperature, sub-cooled boiling can occur that forms porous corrosion-related unidentified deposit (crud).

Crud can cause several problems during normal operational periods. For example, if boron in the coolant reacts with crud, the resulting compound will absorb neutrons, thereby causing a problem related to neutron flux termed axial offset anomaly or crud-induced power shift (CIPS). In addition, crud may cause issues concerning the corrosion mechanism. As previously mentioned, crud is porous, and therefore corrosive solutions can permeate into its pores. If these solutions remain for an extended period of time, crud-induced localized corrosion may occur.

To mitigate these problems, a crud-resistant coating on the fuel cladding was applied in this work using a material, titanium nitride (TiN), known to reduce the van der Waals force between crud particles and the coated surface as compared to commercial zirconium alloy cladding [2]. Heat flux and water chemistry conditions were first set using several numerical calculations and normal PWR operation conditions, and then crud sources such as Ni and Fe ions were injected at highly saturated concentrations in the experimental setup following the results of preceding research [3]. To generate sub-cooled boiling on sample surfaces, a rod-type heater was used.

## 2. Experimental

### 2.1 Experimental Conditions

Crud adhesion experiments were conducted under the typical water chemistry conditions inside a PWR primary circuit. To generate sub-cooled boiling on heated sample surfaces, a rod-type heater was used. The target surface temperature of the rod heater was set to 346 °C, which, as mentioned in the previous section, fits

the sub-cooled boiling condition at 15.5 MPa and satisfies the IAEA regulation for cladding surface temperature.

### 2.2 Metal Ion Injection

There are three means to inject a metal source: metal powder injection, extra metal autoclave installation, and metal ion solution injection. Among them, the metal powder method can agglomerate and lead to a flow path blockage, and with the extra metal autoclave installation method, one cannot control the exact amount of metal ions. Therefore, this study adopted the metal ion solution injection method.

In a commercial nuclear power plant, the Ni and Fe ion concentrations in the coolant are strictly controlled to be under ppb levels. In this study, these concentrations were increased up to a ppm level to accelerate crud deposition. The concentration of each ion was set following a technical report by the Electric Power Research Institute (EPRI) [3] in which the average crud thickness was 0.091 mm and the average porosity was 60 % from a Westinghouse advanced loop tester (WALT) experiment. The crud consisted of NiFe<sub>2</sub>O<sub>4</sub> and nickel oxide (NiO) in a ratio of 56.5/43.5.

In the current study, the required Ni and Fe ion concentrations were calculated from these previous results with consideration of the current experimental loop specifications. It is supposed that crud will deposit on the sample at the upper half of the rod heater, namely over 150 mm of the total 300 mm heated zone length, and it is also supposed that the crud will adhere with the same thickness, porosity, and ratio of chemicals as the result of the WALT experiment. Accordingly, the Ni and Fe ion concentrations used in this work were 24.82 and 11.75 ppm, respectively.

### 2.3 Crud-Resistant Coating

To mitigate crud adhesion on the tube surface, a TiN coating material was chosen to reduce the van der Waals force between the coating and the crud particles as compared to that with a zirconium alloy tube [2].

The TiN was coated on the tubes using the physical vapor deposition (PVD) method in a vacuum state. To measure the coating layer thickness, a sample coated tube was cut into a 1-cm piece and mounted for observation with a scanning electron microscope (SEM). The thickness of the TiN layer was approximately 2.51 μm. The SEM observation result is shown in Fig. 1.

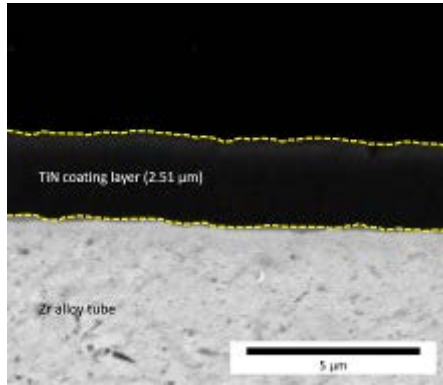


Fig. 1. SEM image of a tube showing the thickness of the TiN coating. Yellow dashed lines are included to highlight the boundary of the TiN.

### 3. Results and Discussion

#### 3.1 U1

The largest crud chunk observed on the surface was chosen for cross-section observation to represent the thickest crud on the sample; Fig. 2 shows a cross-section image. A thickness measurement and cross-section morphology observation were conducted using FIB-SEM. The crud was cut using a focused ion beam from the outer surface up to the zirconium alloy substrate. The thickness of the porous crud was measured at 20 different points and averaged. The maximum and minimum thicknesses were approximately 9.28  $\mu\text{m}$  and 4.60  $\mu\text{m}$ , respectively, with an average was 6.42  $\mu\text{m}$  and a standard deviation of  $\sigma=1.56$ . The sizes of the crud particles near the heated surface were relatively larger than those of the particles of the outer crud layer. This follows from the way crud particles agglomerate, as the particles near the heated surface grow larger as a result of a longer period of heat flux as compared to outer particles.

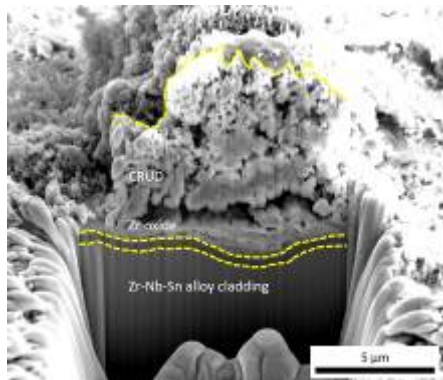


Fig. 2. SEM cross-section image of the sample in experiment U1 showing crud thickness as well as the size variation of crud particles.

#### 3.2 U2

A crud chunk with a diameter of approximately 180  $\mu\text{m}$  was selected for cross-section observation, as shown in Fig. 3. The same observation, cutting, and measurement methodologies as experiment U1 were followed. The maximum crud thickness from experiment U2 was approximately 91.08  $\mu\text{m}$  with a minimum thickness of 82.45  $\mu\text{m}$ . The average was 86.37  $\mu\text{m}$  with a standard deviation of  $\sigma=2.10$ , demonstrating a 13-times increase in thickness compared to the U1 results. According to this thickness difference, it can be noted that the crud fouling rate increased rapidly when the crud deposited on the whole surface of the tube sample. Previous research has also reported a negative fouling rate at early stages as caused by enhanced heat transfer [4,5]. According to these reports, at the beginning of the fouling stage, early deposit enhances heat transfer, which decreases the heated surface temperature. Thus, the fouling rate remains negative for about 1 week but then increases rapidly after the fully deposited state; this was apparent in the current U2 sample case, with 86.37  $\mu\text{m}$  thick crud. The porosity and crud particle size also increased compared to those in experiment U1.

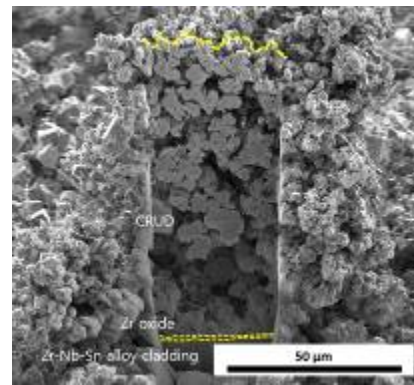


Fig. 3. SEM cross-section image of the sample in experiment U2 showing about 86.37  $\mu\text{m}$  thick, highly porous crud. Particle size decreases with increasing distance from the heated surface.

#### 3.3 T1

The crud was cut to investigate the cross section from the outer surface of the crud down to the zirconium alloy substrate through the TiN-coating layer. The major difference between experiments U1 and T1 is the existence of the zirconium oxide layer that formed immediately above the tube surface in U1. In the case of the TiN-coated tube, the maximum crud thickness was 5.89  $\mu\text{m}$  and the minimum was 2.80  $\mu\text{m}$ . The average was 4.24  $\mu\text{m}$  with a standard deviation of  $\sigma=0.84$ . Because of this crud thickness reduction, the outermost crud particle size from the TiN-coated tube was larger than that from the uncoated sample.

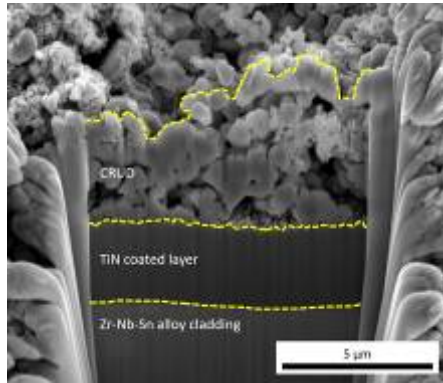


Fig. 4. SEM cross-section image of the sample in experiment T1 showing crud thickness and particle size with no zirconium oxide layer.

### 3.4 T2

Cross-section observations were conducted of the biggest crud chunk from T2, which had a diameter of about 50  $\mu\text{m}$ . When the crud sample was cut vertically, the thickness of the crud was found to be remarkably thinner than the U2 result; while the uncoated sample after 2 weeks showed an average thickness of 86.37  $\mu\text{m}$ , the maximum and minimum thicknesses in T2 were about 5.37  $\mu\text{m}$  and 2.76  $\mu\text{m}$ , respectively. The average crud thickness was about 4.06  $\mu\text{m}$  with a standard deviation of  $\sigma = 0.81$ . This large discrepancy between U2 and T2 is believed to be because crud deposition did not advance to the later stages with increased vertical growth in T2, evidenced by the crud not covering the whole surface in this case. This is supported by the fact that the thickness in T2 was similar to that in T1, indicating that crud starts to grow vertically only after full horizontal coverage of the cladding surface.

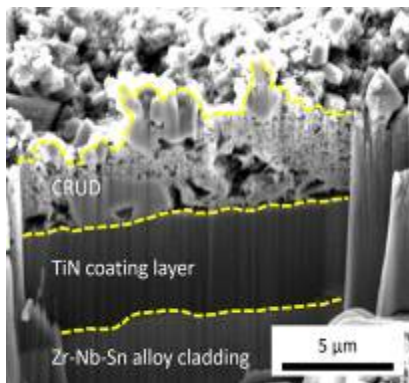


Fig. 5. SEM cross-section image of the sample in experiment T2 showing a thinner crud deposition layer than U2.

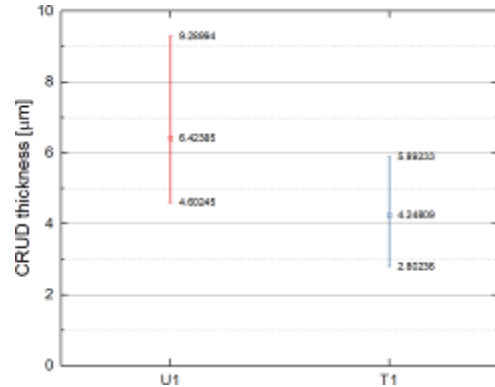


Fig. 6. Crud thickness comparison between experiments U1 and T1.

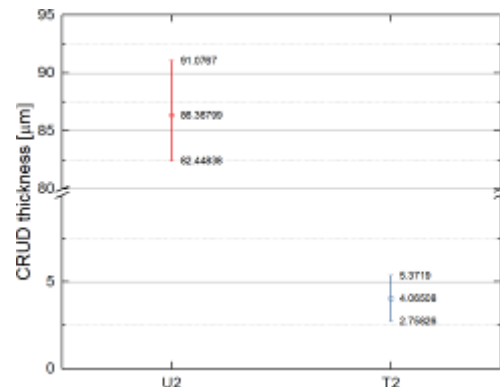


Fig. 7. Crud thickness comparison between experiments U2 and T2.

Crud-resistant coating effects were investigated by first comparing the crud thickness differences between experiments U1 and T1 and between experiments U2 and T2. According to the plotted results in Figs. 6 and 7, crud-resistant coating worked well compared to the uncoated zirconium alloy tube, as the total crud thickness deposited on the tube surface decreased following TiN coating. This crud adhesion resistivity may be caused by a decrease in the van der Waals force between the crud particles and the tube surface material [2].

The crud thickness greatly increased when comparing U1 and U2 cases. This may be caused by the enhanced heat transfer effect that governs heat flux at the early stage of deposition [4,5]. Therefore, after the covering the whole surface of the sample, as in the U2 experiment, the fouling rate increased rapidly enough to ultimately result in a crud thickness of about 13 times that of the U1 experiment. However, in the case of the TiN coated samples, both T1 and T2 remained in the early stage of fouling; the effect of enhanced heat transfer lead to only dispersed coverage, which prevented the crud in the T2 experiment from growing as much as the U2 experiment case.

## REFERENCES

- [1] J.A. Sawicki, Evidence of Ni<sub>2</sub>FeBO<sub>5</sub> and m-ZrO<sub>2</sub> precipitates in fuel rod deposits in AOA-affected high boiling duty PWR core, 374 (2008) 248–269. <https://doi.org/10.1016/j.jnucmat.2007.08.014>.
- [2] I. Dumnerchanvanit, N.Q. Zhang, S. Robertson, A. Delmore, M.B. Carlson, D. Hussey, M.P. Short, Initial experimental evaluation of crud-resistant materials for light water reactors, J. Nucl. Mater. 498 (2018) 1–8. <https://doi.org/10.1016/j.jnucmat.2017.10.010>.
- [3] M. Deshon, J and Wang, G and Byers, A and Young, Simulated Fuel Crud Thermal Conductivity Measurements Under Pressurized Water Reactor Conditions, EPRI, Palo Alto, CA. 1022896 (2011).
- [4] C. Shen, C. Cirone, L. Yang, Y. Jiang, X. Wang, Characteristics of fouling development in shell-and-tube heat exchanger: Effects of velocity and installation location, Int. J. Heat Mass Transf. 77 (2014) 439–448. <https://doi.org/10.1016/j.ijheatmasstransfer.2014.05.031>.
- [5] S.M. Peyghambarzadeh, A. Vatani, M. Jamialahmadi, Application of asymptotic model for the prediction of fouling rate of calcium sulfate under subcooled flow boiling, Appl. Therm. Eng. 39 (2012) 105–113. <https://doi.org/10.1016/j.applthermaleng.2011.12.042>.